**International Journal of Mining Science (IJMS)**
*Volume 7, Issue 2, 2021, PP 10-19*
*ISSN 2454-9460 (Online)*
*DOI: http://dx.doi.org/10.20431/2454-9460.0702002*
*www.arcjournals.org*

# Dynamic Interaction and Slide Properties of a Bent Hoisting Wire Rope in a Hard Rock Mine: Maddhapara Hard Rock Mine Case Study

**Mohammad Forrukh Hossain Khan[1], Mahfjur Rahman Jinnah[1,2], Md Mehedi Hasan [1], Md. Rubayet Hasan [1,2]**

[1] *Department of Petroleum and Mining Engineering, Faculty of Engineering & Technology, Jashore University of Science and Technology, Jashore 7408, Bangladesh*

[2]*Germania Corporation Ltd. Maddhapara Hard Rock Mine, Bangladesh*

***Corresponding Author:** **Mohammad Forrukh Hossain Khan,** *Jashore University of Science and Technology, Jashore 7408, Bangladesh*

**Abstract:** *Throughout this research, the contacting and sliding properties of a twisted hoist cable in a hard rock mine have been examined to see how they change with time. By combining lifting mechanics with frictional propagation concepts, it was possible to measure the structural features of lifting cable bends over frictional lines at several different arc points. Using a finite element analysis of interacting bent ropes and frictional liner, researchers were able to investigate the cohesion and, friction features and comparative slide capacitances between some of the ropes and the frictional liner as well as between contact strands throughout the cable. The findings demonstrate that the dynamical stresses of bent cables at various arc positions are linked to the slide and dormant slip stages of cable sections. At every central angle and at every lifting time, higher stress concentrations are observed at interacting sites between consecutive strands and between the cable and the frictional liner, as well as at interacting sites between the cable and the frictional lining. Enhanced equivalent von Mises stress proportions on the wire cross-section and close interaction places inside the vertical displacement between both the wire and tension wrapping result from an increment in the line parallel, as the angle of rotation is raised, as contrast to when the angle of rotation is decreased, consistent stress - strain concentrations in within active slip angle occur. A relative slip is caused by differences between the strained relations of a bent wire section on both edges of the vertical displacement, as opposed to no relative slip occurring on either edge of the inactivated vertical displacement. The wire section comes into contact with the tension lining or with neighborhood strands.*

**Keywords:** *Bent Hoisting Rope, Hard Rock Mine, Rope, INTROS Machine, Hoisting Pulley*

## 1. INTRODUCTION

In hard rock mines, the friction hoist is used to uplift the tools, workers, and coal which also associate underground with the ground. Hoisting rope is considered a transmission element in any kind of mine. The structured and secure functioning of the hoisting system has prominent importance all over the world in any kind of mining design. Vicious disasters occur through the rupture failure of the raising rope which damages the safety condition of a mine [1]. The frictional system of hoisting is comprised of straight-line and bent sections. In its internal steel wires bending stresses are generated that are brought up by the bent rope throughout the friction pulley. Rope tensions fluctuation is represented at different phases (constant speed, acceleration, deceleration) at the time of lifting. [2].At different, friction pulley of the central angles on the positions of rope segments regulate the bending stress of the rope for the time being [3].

At the time of uplifting bent, rope prompts bending fatigue of the rope which is also assigned to cyclic bending stress [4]. In between contacting wires, contact load and relative slip are occurred by the bending fatigue of the rope. Consequently, it causes fretting fatigue throughout the neighboring wires [5].For the time being throughout the friction pulley, the damages in between the friction lining and rope are occurred due to the elastic deformation. Moreover, the elastic deformation of the cable is subjected to twisting exhaustion[6]. Lastly, fatigue and wear fracture of rope wires has lessened the safety and lifetime of the rope which is attributed to those interior and outside damages of cable.

Hence, the twisting fatigue destructive characteristics of the rope, dynamic contact, and slip characteristics among the bent rope and friction alliner as well as in between connected strands of bent hoisting rope are substantially crucial.

Several studies on rope bending characteristics have been carried out by numerous researchers under the element of bending stresses of rope on a mine. Chen et al.[7] have analyzed the stress properties of the rope. Therefore through the friction pulley, [8, 9] and [3] have analyzed the tensile stresses of the bent rope. Bending stress under the radial force has been investigated by Yu et al. [10]. In the elevator throughout the leading pulley, the contact pressure in between wires of the bent rope has been exhibited in the studies of Sasaki et al [5]. Whereas in steel wires of the bent rope, Knapp [11] has been estimated the compound pressure. Contact forces between connected wires as well as the pragmatic equation of slip strokes have been suggested by[5, 6]. The mechanical configuration of the rope strand is determined in the study of [12] which is affected by the coupled role of pull, torsion, and bending. In steel wire rope, [13] have estimated bending cyclical stress. In addition, on wire rope bending the effect of deterioration and damaging grade over sheave fatigue tolerance has also been studied by [14].Still, at the time of dynamic hoisting with fluctuating tensions, dynamic contact and slippage of cable properties between the bent rope and friction lining as well as in between contacting strands of the bent rope have not been described.

The main scheme of this current study is an analysis of dynamic contact and slip properties of bent raising cable in a hard rock mine. At different locations, dynamic tensions of bent raising cable have been determined in different locations of the rope. Meanwhile, the stress distribution of dynamic contact has also derived among communicating strands of bent cable and in between the bent rope and friction lining. There have been also shown extreme relative slips between the bent able and frictional lining and among strands of bent cable.

## 2. MATERIALS AND METHODS

### 2.1. Field Investigation of Rope Test

The intros machine version 7.5.3 E was fixed on the corner of the rope which was being tested. Then the rope is up and down and the full rope is magnetized. Then the data is collected. The machine display shows the percentage rate of the roping system. As illustrated in Fig. 1, the lifting cable in a frictional hoisting process is the selection of horizontal

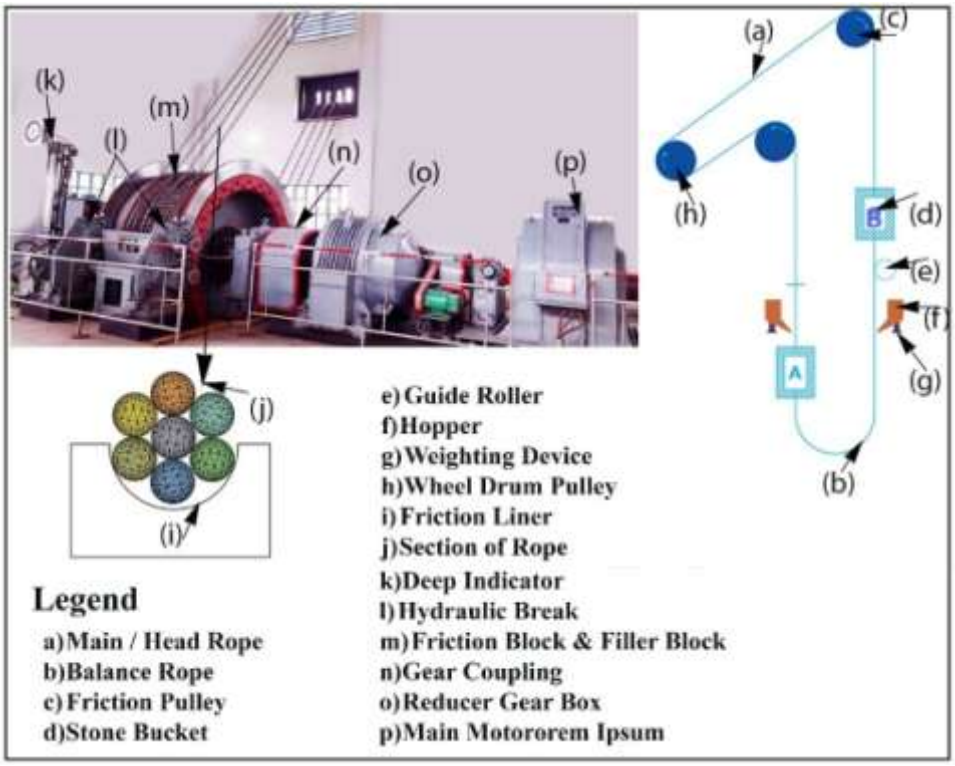


**Fig1**. *The frictional hoisting mechanism at a hard rock mine is shown in this diagram.*

## 2.2. Dynamic Stresses of Twisted Hoisting Ropes with Different Tensions

*2.2.1. Hoisting Rope Dynamic Stresses during Transitional Portions*

In the studies, the construction of steel rope 6V×34+NF having a diameter of 31mm is selected. Rope dynamic tensions in both sheave tangents have been calculated using the Eqs. (1) and (2) and using software MATLAB simulations based on the hard rock mine hoist settings and cable parameters listed through Tables 1-5, [1].

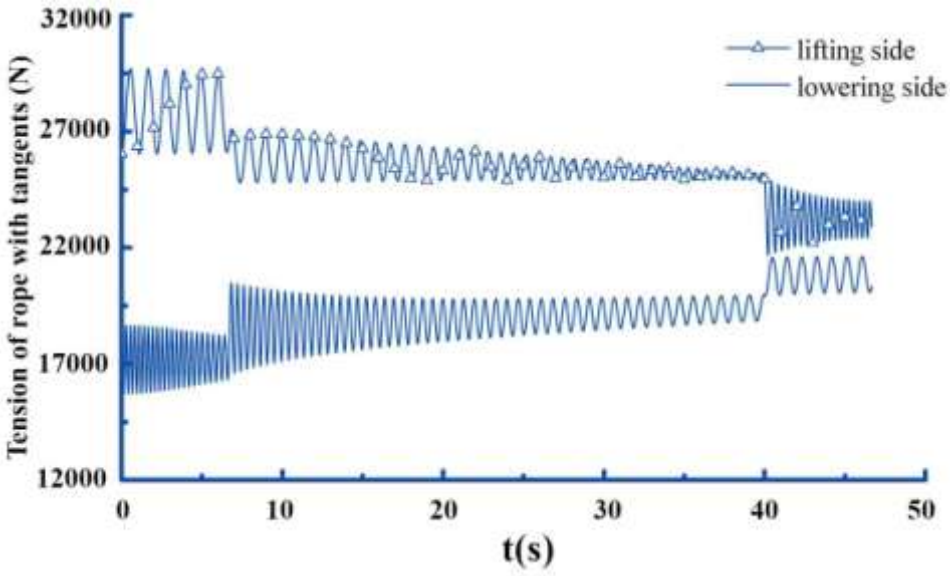


**Fig2.***Sheave tangents on both the raising and lowering sides create stress in the wire rope.*

Fig.2 depicts three conditions changing of ascending and falling tendencies of cable tensions at the dropping and exciting sides, as well as the lowering and raising sides.

$$\ddot{S}_1 = [E \times A \times (g + a) - (E \times A / (m_1 + \rho \times L_1/ 3 + a) \times S_1 - 2 \times v \times \dot{S}_1) / L_1 \quad (1)$$

$$\ddot{S}_2 = [E \times A \times (g - a) - (E \times A / (m_2 + \rho \times L_2 / 3) + a) \times S_2 - 2 \times v \times \dot{S}_2) / L_2 \quad (2)$$

Where E is the steel rope elastic module, MPa, A is the number of cross section of total cables, $mm^2$, $m_1$and $m_2$ is the command line mass on the raising and lowering of the sides (in the current study, 27000 and 17000kg), g is the acceleration of gravity, $m/s^2$, ρ is the rope mass,kg/m, a is the acceleration and deceleration during stone bucket lifting, $m/s^2$, v is stone bucket lifting speed, m/s,$L_1$ and $L_2$ are spacing between Sheave tangent and stone bucket, m, $S_1$ and $S_2$are tensions on the steel rope at sheave tangents on raising and lowering sides, consistently, N.

Fig.3 has illustrated a rope with a wrap angle, $\alpha = \pi$, the rope is looped across the cylinder shaped frictional rope. The frictional line is fastened between the pulley and the steel rope. $S_1$ and $S_2$, are tensions for the rope at the left and right sheave tangents (on the raising and lowering sides), respectively. When the steel rope tension, $S_1$, rises to create the imminent total slip of the rope over the friction lining,$S_1$, and $S_2$ rope tensions, the Euler formula as stated by Eq (3).

$$S_1 = S_2 e^{\mu\alpha} \quad (3)$$

where μ indicates the continuous frictional coefficient among the steel rope andfrictional liner. The steel rope distance doesn't fulfill the total slip condition, i.e.$S_1 < S_2 e^{\mu\alpha}$, during the actual lifting. The wrapping angle is a slip angle, $\gamma$; and the angle of inactive slip, $\lambda$, has been revealed in Fig. 3. The angle of slip and inactive angles of slip has given inEqs. (4) and (5). The strength of the steel rope is determined by Eq. (6)[15] across the contact area.

$$\gamma = 1 / \mu . \ln (S_1 / S_2) \quad (4)$$

$$\lambda = \pi - \gamma \quad (5)$$

$$F(\varphi) = \begin{cases} S2, & 0 < \varphi < \lambda \\ S2 \cdot e^{\mu(\varphi - \lambda)}, & \lambda < \varphi \leq \pi \end{cases} \quad (6)$$

Where $\mu$ is considered to remain constant throughout the contact area during lifting, i.e., $\mu$ = 0.28 in this research, and F ($\varphi$) is the bent cable of the tension at the frictional pulley's essential part $\varphi$.

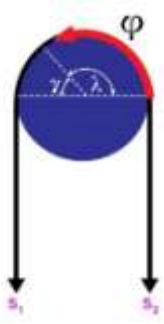


**Fig3.** *Schematic illustration of frictional transfer between the steel rope and frictional lining surrounding friction head pulley.*

## 3. RESULT AND DISCUSSION

### 3.1. Bending Rope Dynamic Stresses at Different Sites

In Sect. 2.1, the dynamic tensions of the steel rope on raising and lowering sides have been replaced by Sect. 2.2 in Eqs. (4) and (5) for slip-on dynamic tension and inactive slip angle of the seam at the time of lifting. Dynamic slip and inactive slip angles have been replaced with Eq. (6) to get dynamic tension of bent hoisting rope portion at separate center angles of the frictional lining pulley.

When comparing the dynamic steel rope stress in the normal spinel area to the continuous wire stress in the zone of slip angle, Eq (6) demonstrates that the stress of dynamic steel rope rises through rising the central angle $\varphi$ in the zone of slip angle. Fig. 4(a) shows the equal dynamic steel rope tension at the central angle degree$\varphi$ = 20°, with the virtually passive slip condition ascribed to $S_2$ throughout (Fig. 5). The complicated fluctuation of tension of the rope as illustrated in Fig. 4(b) is induced by combination slip and inactive slip statements at the angle of the central part$\varphi$= 180° (Fig. 5). The total tension of the rope in Fig. 4(c) at central angle $\varphi$ = 140° as $S_1$ at central angle $\varphi$ = 180° livers, owing to the near slip condition throughout. Centrally angled 20°, 80° and 140° wire tension variations vary between312-343, 321-345, and 335–346kN, respectively.

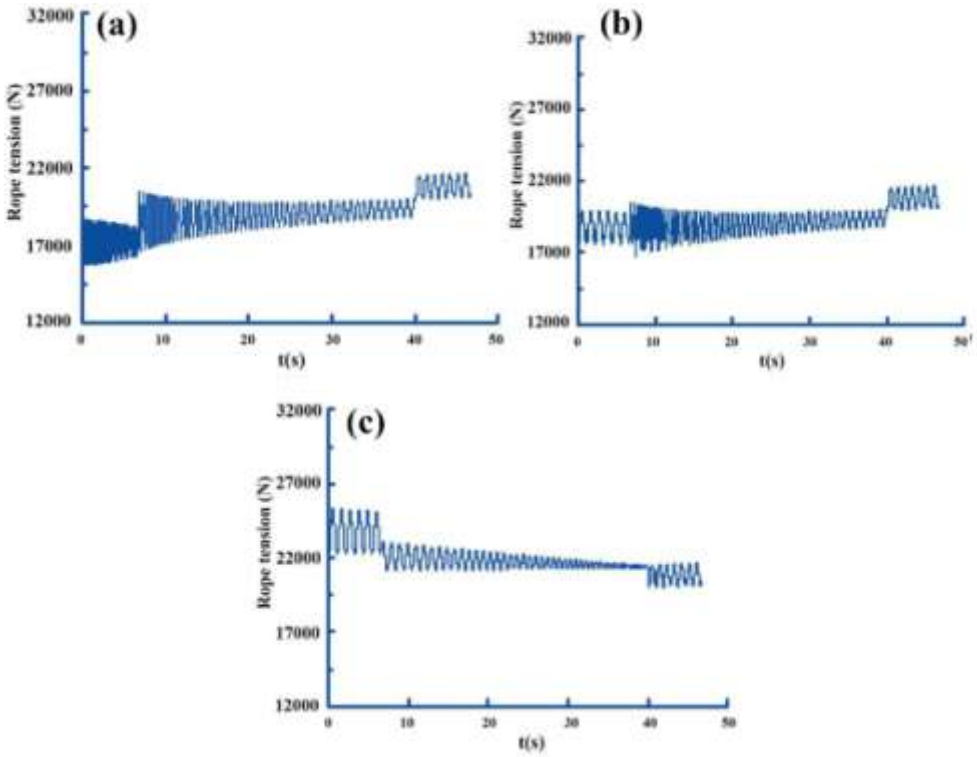


**Fig4.** *The rope tension is measured at various center angles. 20°, 80,° and 140°*

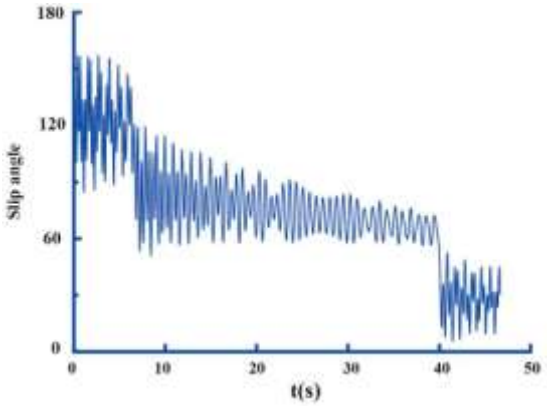


**Fig5**. *The slip angle between both the cable and frictional liner increases.*

### 3.2. Connecting Bent Wire and Frictional Lining Based on Finite Element Analysis

#### *3.2.1. Design and Manufacture of Communicating Bent Ropes and Frictional Linings*

The complicated spiral shape and a significant quantity of calculations homogenize the strands in the seam to simplify the wire rope structure, thus reducing the computation time and ensuring computational convergence. It is necessary to use Sketch Up 2014 to build the model of the geometric shape of the contact bent wire rope and the frictional lining has been represented in Fig. 6. It is 250mm inlay length and 600 mm in friction pulley diameter, with the diameter of the friction pulley being 128 mm. Throughout the geometric shape, the bending cord is 250 mm long and the bottom surface of the frictional liner has a curving radius of 600 mm. The geometric model has been loaded into ANSYS 2020 WORKBENCH.

**Fig6**. *Model of connecting bent rope and frictional lining in three dimensions.*

#### *3.2.2. Properties of Material and Physical Discretion*

The commercial structural analysis program was utilized in this study. Completely all strands have been constructed using the same isotropic material. Due to its complicated structure and CPU constraints, the cord has been evaluated using the elastic material method. The modulus of Young is 193GPa and the ratio of Poisson is 0.305. Fig. 7 has shown the numerical simulation models for the cable and the fractional coating, respectively. The apertures were satisfactory at the contact points between neighboring sections. The wire element of meshed with 684,702 and nodes 809,509. The rope has meshed applying 16,709 components and 85,786nodes. Every junction has three main components, namely, the capacity to travel in the X, Y, and Z directions (U1, U2, U3).

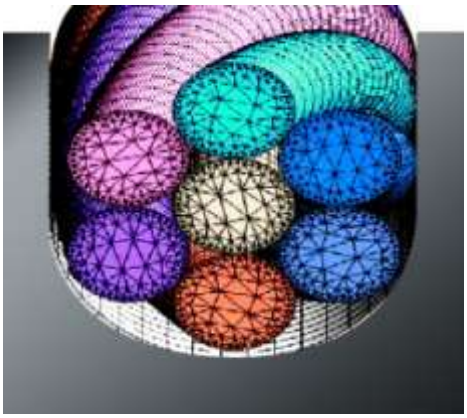

**Fig7.** *Mesh of finite elements.*

*3.2.3. Interactional Characteristics*

This method was utilized to describe the interface region connections among connecting strands, as well as the relationships among touching bent wire ropes and the frictional coating applied to the contact area in ANSYS 2020 WORKBENCH. Analysis of frictionless elastic connections among spiral segments in the ropes as well as friction elastic connections among the wire and the frictional lining (coefficient of friction = 0.23) [3] has been carried out.

*3.2.4. Restriction and Bounding Situations*

The tension of ropehas been achieved with the Segment. 2 approaches. The pressures on the cable at various center angles correspond to the intermediate period of every step of lifting that has shown in Table1 (acceleration, constant speed, deceleration). Static support was provided to the frictional coating, and wire tensions have usedforeach ends parts of the wire as indicated in Table 1. The assumption in the research [13]was that the cable border would stay flat, and then reference points were utilized to link nodes on the appropriate cross-sectional parts.

**Table1.** *Tensions in the steel wire rope at various center orientations and at various raising times*

| Raising Time (s) | Central angle 20° | | Central angle 80° | | Central angle 140° | |
|---|---|---|---|---|---|---|
| | Tension F1 (N) | Tension F2 (N) | Tension F1 (N) | Tension F2 (N) | Tension F1 (N) | Tension F2 (N) |
| 4 | 27,227 | 37,227 | 30,847 | 30,847 | 31,788 | 31,788 |
| 24 | 33,456 | 33,456 | 31,789 | 31,789 | 32,543 | 32,543 |
| 44 | 34,766 | 34,766 | 34,766 | 34,766 | 35,962 | 35,962 |

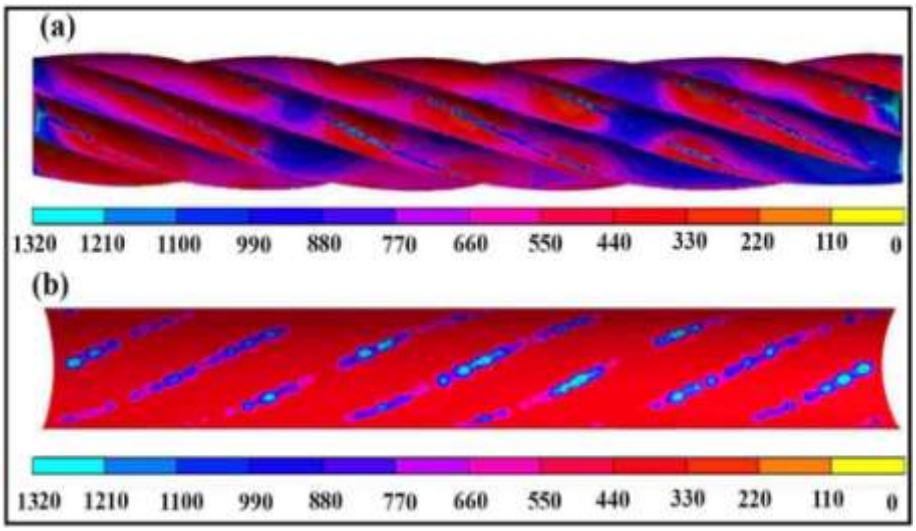


**Fig8**. *The frictional lining and the cable are subjected to friction tension.*

## 4. Characterization Dynamic Contact Qualities between Both the Rope and the Friction Lining.

### 4.1. Characterization of Contact Stress of Rope

Contact pathways and friction linings of a rope have been formed by spiraling contact paths and friction linings are shown in Fig. 8, which is due to the helical form of the cable. The bending, tension, and contacts between the cable and the frictional lining all contribute to creating the complicated stress distribution pattern of the cable. However, the stress distributions on the surfaces of the strand and frictional liner are greater throughout the interaction route than they are at other places, indicating that perhaps the surfaces are more stressed.It is seen that contacting conditions between both the cable and frictional lining exhibit active slip situations at $\varphi$= 20° during raising time 4 seconds and at $\varphi$ = 20° and $\varphi$ =80° during raising time 24 and 44 seconds, respectively. This results in an increase in the value of F1 over F2. This increases the raising period to generate a higher total cable tension of $\varphi$ = 20° pounds and $\varphi$ =80 °pounds (Table 1). This produces more stress distribution between both the cable and the frictional line (dQ = 2F sin (dh/2))[16].

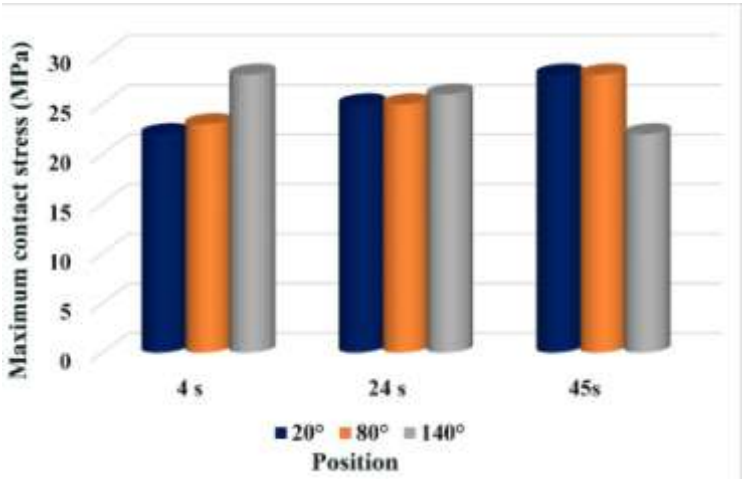


**Fig9.** *Amount of shear stresses that may exist between the cable and the frictional lining*

Throughout the formula, dQ indicates the friction coefficient between each section of cable and the frictional line, N, F implies equal stresses from both edges, N, and dh represents the center angle within each section of cable across the contact pulley, N. Fig. 9 indicates that stress distribution decreases with the increasing period when $\varphi = 140°$, that has ascribed to a general reduction in the amount of cable stress. The total symmetrical equal of Mises stress ranges on cable cross-sections and larger maximum tensile ranges at connection points between neighboring segments and strands and frictional lines are shown in Fig. 10 and Fig. 11,at any center altitude, showing tensile stress in close points of contact. Conflicts of the bent wire section on both edges result in greater comparable stress and strain near attempting to contact places among S0 and S1 fragments, between S1 and S3 fragments, and between S4 strand and friction liner, resulting in higher tensile stress and more major damage to the wire section and vibration line. Greater maximum stress concentrations can be readily observed in Fig. 11, which depict three connecting pathways on the S4 segment interface and six connecting pathways on the S1 strand surface, respectivelywhere greater maximum stress concentrations are visible.

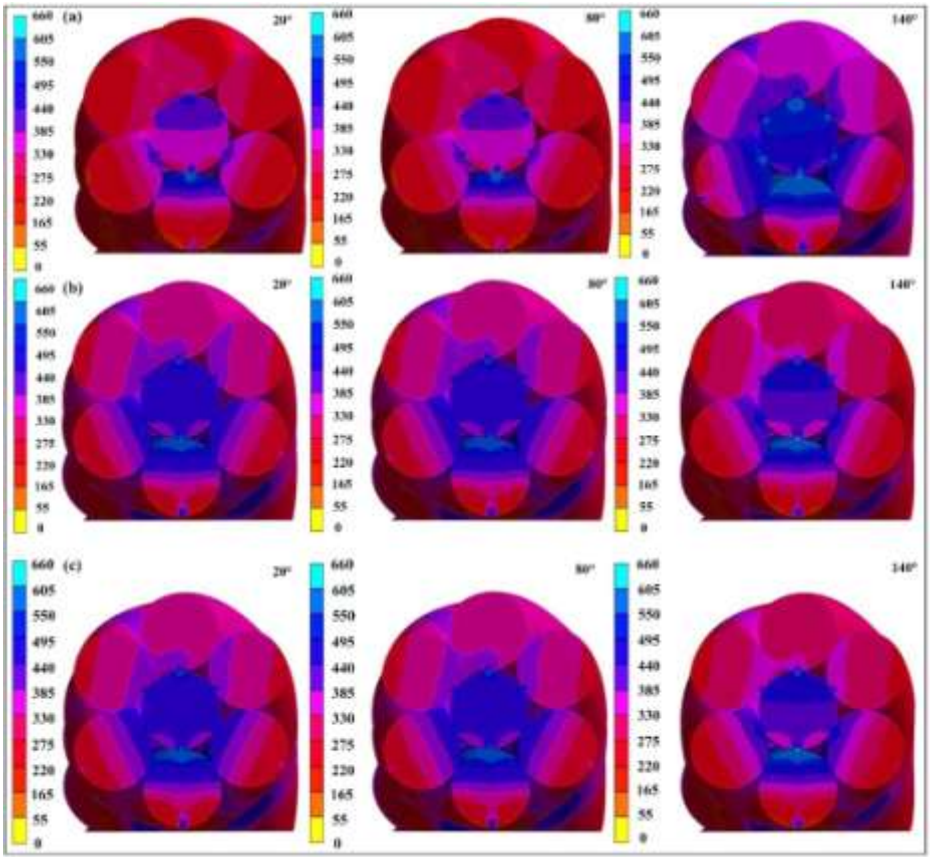

**Fig 10**.*(a) 5 s, (b) 24 s, and (c) 44 s comparable von Mises stress patterns on cable cross-sections*

With increasing hoisting period and within the drop diffraction angle $\varphi$ between both the wire and vibration filling, a significantly raised central angle $\varphi$ results in overall greater comparable von Mises stresses on the rope bridge and near attempting to contact areas, which are traced back to overall greater conflicts on both sides, including the wire section. Due to continuous cable tensions, a rise in the line parallel $\varphi$ produces consistent comparable von Mises physical demands across the cable cross-sectional area and nearby contacting sites.

The highest contact tensions among straight and spiral strands are 514.9, 605.8, and 467.3 MPa at raising periods of 4, 24, and 44s, respectively; the greater contact strains between adjacent spiral strands are 502.0, 495.5, and 482.1 MPa at raising times of 4, 24, and 44s, respectively. An improvement in lifting occurs at a certain center angle u. Because of increased rope strained relations on both sides of the wire section in the cases of central angles of 20° and 80°, this results in a considerable enhanced comparable stress concentration on the wire trans and near contacting areas on the rope section, as opposed to decreased stress values dividend payments in the case of credited to overall lowered wire tensions on both edges of the wire section. The greater contact stresses between straight and spiral strands are 568.6, 468.6, and 513.9 MPa at center angles of 20°, 80°, and 140°, respectively; the greater contact stress and strain between adjacent plain strands are 482.14, 482.14, and 502.0 MPa at center angles of 20°, 80°, and 140°, respectively.

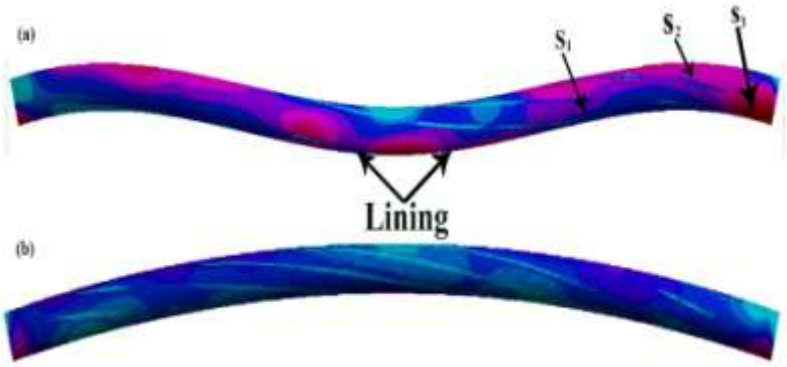


**Fig11**. *Von Mises stress patterns for segments $S_1$and $S_3$*

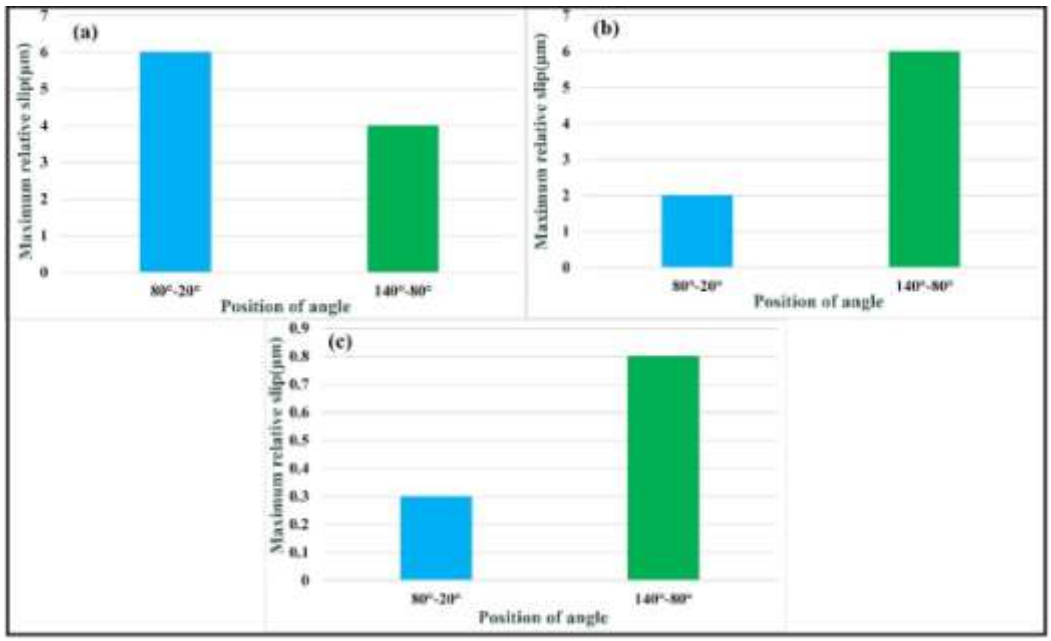


**Fig12.** *Slip times between the cable and frictional lining are as follows: (a) 4s, (b) 23 s, and (c) 44s.*

### 4.2. The Features of Relative Slip

Three raising periods result in an angle of friction between both the cable and the frictional liner that measures 628 meters in thickness, and the cable section between connection to detachment of the frictional liner has a length limit of 0.25 seconds. Because of the limited contact period between the

rope segment and the contact surface, it is anticipated that F1 and F2 remain static throughout the reforming process. Generated by the displacement of the cable as a result of stress variations both at endpoints, the slippage between both the cable and frictional liner may be seen. Therefore, when F1 = F2, the dormant slip condition between both the cable and frictional line is induced between the two variables. There have been no comparative slippage matching to dormant slip angles at hoisting times of 24 and 44 s, which corresponds to center angles 20°–80°, as shown in Fig. 12a. At raising period 4s throughout velocity, the average maximum pulls among wire and tension liner are 4.9 lm at center directions 20°–80°, and 2.9 lm at center directions 80°–140°, (Fig. 12b respectively; the greatest average slip, i.e. 4.3 lm at main directions 80°–140°, is visible at hoisting period 24 s throughout consistent speed point (Fig. 12c); and the smallest comparative slip, i.e. 2.3 lm at main directions 20°–80°, is visible at hoisting period. Following deceleration, the largest relative slippage is 0.3 lm at middle degrees 80°–140° at a hoisting period of 44 s at middle degrees 80°–140°. Very tiny comparative slides occur throughout deceleration as a result of modest variations in the stresses of the wire section on each side of the vehicle.

The amount of comparative slip magnitude is equivalent to the difference between displacements of adjacent sections at different center degrees at any given raising period. According to Fig 12and 13, the greatest relative slippage among interacting strands at main degrees of 80° and 140° degrees, and central degrees of 80° and 20° degrees, may be achieved at different lifting times at central degrees of 80° and 20° degrees. It can easily be shown that the highest mean slippage among regular and spiraling strands, as well as the highest mean slippage among spiraling wires, both shows change the laws that are quite equivalent to the highest mean slippage between the cable and frictional material.

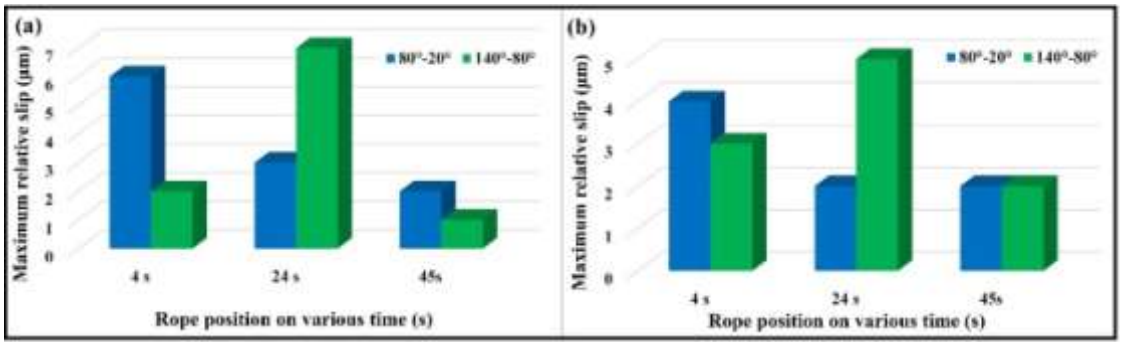


**Fig13**. *Spiral strands with the greatest amount of comparative slip*

(Fig.13a and b) demonstrate that the highest mean slippage among contacting segments at center angles of 80° and 20°, i.e. 2.9 and 2.1 lm, is greater at 4 s than the highest mean slippage among encountering segments at middle angles of 80° and 140°, i.e. 1.1 and 1.5 lm. But on the other hand, on Fig.13a, the highest mean pulls here between able to contact strands at main angles of 80° and 20° are both equivalent to 0 at 24 seconds and 44 seconds, respectively, which can be contributed to equal displacements of wire strands caused by equivalent rope tensions in the dormant normal spinel region at 24 seconds and 44 seconds, respectively. As shown in Fig. 13b, the greatest relative slippage between plain and spiral sections at middle angles of 80 and 140 degrees is 2.9 and 3.8 lm, respectively. In Fig. 13, the greatest relative slippage among spiraling sections is 2.1 and 2.6 lm, respectively, for middle points of 80° and 140° degrees (as indicated in the figure), respectively.

## 5. CONCLUSIONS

Energetic tensions of curving wire in a mine at various arc places have been determined using lifting interaction and friction transmitting hypotheses, as well as experimental data. Contact stresses and comparative slips among notifying elements (among loop strands, among normal and ripple strands, between both the wire and friction liner) have been calculated using a finite element analysis with flexible conflicts as initial conditions.Various channel dimensions of the vibration pulley produce different dynamic conflicts of bent wire sections, but they all produce 3 types that fluctuate. Various elevator times produce different results external opportunities here between the wire and the tension lining, resulting from different slip angles. Compared to other areas, the interaction particles between both the wire and the tension trying to line possess increased stress dividend payments along the communication direction than other places. Lifting times and main edges that differ from one another

effect of different highest stress concentrations between the wire and tension trying to line. With the rising hoisting moment, the maximum contact stresses among neighboring strands in the twine reduction in magnitude. With growing line parallel in the nonactive normal spinel region, the greater contact impacts among adjacent strands remain constant at higher line parallel. Compared to the inactivated normal spinel area, greater contact stress and strain among neighboring strands have greater yields when they are in the normal spinel region with active vertical displacement. A significant rise in the raising period results in a reduction in the normal spinel area. The highest mean slips between both the wire and the tension lining, as well as the highest mean slips among notifying layers, are 5.3 and 4.8 meters, in both.

## REFERENCES


[1] Wang, D., D. Zhang, and S. Ge, Effect of terminal mass on fretting and fatigue parameters of a hoisting rope during a lifting cycle in coal mine. Engineering failure analysis, 2014. 36: p. 407-422.

[2] Wang, D., et al., Effect of various kinematic parameters of mine hoist on fretting parameters of hoisting rope and a new fretting fatigue test apparatus of steel wires. Engineering Failure Analysis, 2012. 22: p. 92-112.

[3] Zhang, J., et al., Tribo-fatigue behaviors of steel wire rope under bending fatigue with the variable tension. Wear, 2019. 428: p. 154-161.

[4] Wang, D., et al., Finite element analysis of hoisting rope and fretting wear evolution and fatigue life estimation of steel wires. Engineering Failure Analysis, 2013. 27: p. 173-193.

[5] Argatov, I., et al., Wear evolution in a stranded rope under cyclic bending: Implications to fatigue life estimation. Wear, 2011. 271(11-12): p. 2857-2867.

[6] Wang, D., et al., Effects of hoisting parameters on dynamic contact characteristics between the rope and friction lining in a deep coal mine. Tribology International, 2016. 96: p. 31-42.

[7] Chen, Y., F. Meng, and X. Gong, Parametric modeling and comparative finite element analysis of spiral triangular strand and simple straight strand. Advances in Engineering Software, 2015. 90: p. 63-75.

[8] Erdönmez, C. and C.E. İmrak, Numerical model for an IWRC bending over sheave problem and its finite element solution. Recent Advances in Computers, Communications, Applied Social Science and Mathematics. Barcelona, Spain, 2011: p. 199-205.

[9] Erdönmez, C. and C.E. İmrak, Modeling and numerical analysis of the wire strand. Journal of Naval Sciences and Engineering, 2009. 5(1): p. 30-38.

[10] Yu, Y., X. Wang, and Z. Chen, A simplified finite element model for structural cable bending mechanism. International Journal of Mechanical Sciences, 2016. 113: p. 196-210.

[11] Zhang, J., et al., Dynamic contact and slip characteristics of bent hoisting rope in coal mine. Journal of the Brazilian Society of Mechanical Sciences and Engineering, 2018. 40(3): p. 1-9.

[12] Foti, F. and L. Martinelli, Mechanical modeling of metallic strands subjected to tension, torsion and bending. International Journal of Solids and Structures, 2016. 91: p. 1-17.

[13] Ridge, I., C. Chaplin, and J. Zheng, Effect of degradation and impaired quality on wire rope bending over sheave fatigue endurance. Engineering Failure Analysis, 2001. 8(2): p. 173-187.

[14] Feyrer, K., Wire Ropes Under Bending and Tensile Stresses, in Wire Ropes. 2015, Springer. p. 179-330.

[15] Wang, D., Dynamic contact characteristics between hoisting rope and friction lining in the deep coal mine. Engineering Failure Analysis, 2016. 64: p. 44-57.

[16] Feyrer, K., Wire ropes. 2007: Springer.


**Citation:** *Mohammad Forrukh Hossain Khan, et.al.(2021)" Dynamic Interaction and Slide Properties of a Bent Hoisting Wire Rope in a Hard Rock Mine: Maddhapara Hard Rock Mine Case Study", International Journal of Mining Science (IJMS), 7(2), pp.10-19, DOI: http://dx.doi.org/ 10.20431/2454-9460.0702001*